Journal of the Korean Physical Society, Vol. 47, No. 5, November 2005, pp. 889∼894

Effects of Tin Concentration and Post-Annealing on the Electrical and the Optical Properties of $In_{2-x}Sn_xO_3$ ($x = 0 \sim 0.25$) Deposited at Room Temperature

J. W. Bae,* H. C. Lee and G. Y. Yeom

Department of Materials Science and Engineering, Sungkyunkwan Univeristy, Suwon 440-746

(Received 6 September 2005)

Indium-oxide thin films were deposited on glass substrates at room temperature by using a dual oxygen-ion-beam-assisted evaporation system, and the effects of the vacuum annealing conditions on the tin-doping efficiency and on the electrical, the physical, and the optical properties of the films were investigated. The resistivity of pure indium-oxide (IO) films increased with annealing temperature while that of tin-doped indium-oxide (ITO) films decreased. The changes in the electrical conductivities of the IO and the ITO films with annealing temperature were due to a decrease in the number of ionized oxygen vacancies and an increase in the ionization probability of neutral tin atom, respectively. Optical transmittances measured using a UV-visible spectrophotometer were higher than 90 % and did not change significantly with annealing temperature. The RMS roughness of the as-deposited films was lower than 1 nm, regardless of the tin percentage, and that after annealing at temperatures below 300 °C was lower than 1.2 nm.

PACS numbers: 81, 78
Keywords: ITO, Room temperature, Annealing, Ion beam, Evaporation

I. INTRODUCTION

Tin-doped indium-oxide (ITO) thin films deposited at room temperature (RT) or low temperature (below 100 °C) have been proposed as transparent conductive oxides for flexible plastic substrates, such as polycarbonate (PC), polyetylene terephthalate (PET), polyimide (PI), *etc.* Several techniques to deposit RT-ITO films, such as evaporation, high-density-plasma-assisted evaporation (HDPE) [1–3], ion-beam-assisted-evaporation (IBAE) [4–9], magnetron sputtering [10–12], ion beam sputtering (IBS) [13–15], and pulsed laser deposition (PLD) [16–18], have been studied. Among these techniques, IBAE is known to be one of the superior methods with high conductivity and high optical transmittance [6–9].

The electrical properties of ITO films strongly depend on the number of ionized oxygen vacancies and the concentration of tin atoms in the films. The former donates two free electrons per vacancy to the donor level through ionization, and the latter donates one electron per tin atom through ionization or remains as a neutral defect, leading to a degradation of the conductivity. Therefore, understanding and controlling the role of the tin atoms existing in the ITO thin films as donors or impurities (defects) must be achieved because ionization of tin atoms is s main key factor in obtaining an indium-oxide film having good electrical and optical properties. In this study, the effects of tin concentration in ITO thin films deposited by using a dual oxygen IBAE technique at room temperature, followed by vacuum annealing, on the electrical and the optical properties of indium-oxide (IO) and ITO thin films were investigated.

II. EXPERIMENTAL CONDITIONS

Amorphous IO and ITO thin films with thickness of 120 nm and different tin concentrations were deposited on glass by using a dual oxygen IBAE system. To obtain different tin concentrations, we used sintered ITO materials containing tin-oxides with tin concentrations of 0, 5, 10, 15, and 25 wt.% as evaporation sources. The deposition system used in the experiment consisted of an electron beam evaporator and two internally mounted oxygen-ion guns. Both of the oxygen ion guns were driven by radio-frequency inductively-coupled-plasmas (13.56 MHz), and two grids were attached for the ex-

*E-mail: jwbae70@gmail.com

traction and the acceleration of the oxygen ions generated in the plasma chamber. The voltages applied to the accelerator and the extraction grids of both guns were +1.2 kV and −100 V, respectively. One of the oxygen-ion guns (ion gun 2) faced the substrate, and the flux was varied by changing the rf power (200 to 400 W) and the flow rate of oxygen (4 to 6 sccm) to obtain the lowest resistivity by optimizing the oxygen content in the film. Optimal conditions for ion gun 2 were an rf power of 300 W and an oxygen flow rate of 4 sccm for IO, an rf power of 300 W and an oxygen flow rate of 5 sccm for ITO with 5 to 15 wt.% tin oxide, and an rf power of 350 W and an oxygen flow rate of 5 sccm for ITO with 25 wt.%. The second oxygen ion gun (ion gun 1) was located near the ITO evaporator and irradiated oxygen ion beam toward the ITO flux, not toward the substrate. The condition of ion gun 1 was fixed at an rf power of 250 W and an oxygen flow rate of 4 sccm.

Annealing of the films was performed in a vacuum of 5 $\times$ 10^{-2} Torr for 1 h, and the temperature was varied from 140 to 300 °C. The properties of the films were evaluated using a four-point probe, a UV-visible spectrophotometer, X-ray photoelectron spectroscopy (XPS), and atomic force microscopy (AFM).

III. RESULTS AND DISCUSSION

Fig. 1 shows the effect of the annealing temperature on the sheet resistance of the films deposited by IBAE with various values of the tin-oxide wt.%. The tin-oxide wt.% in the ITO source was varied from 0 to 25 wt.%, and the rf power and the oxygen flow rate to ion gun 2

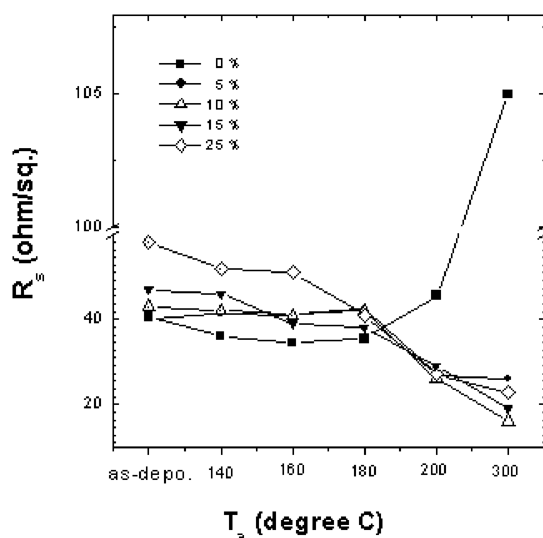

Fig. 1. Effect of tin-oxide wt.% in the ITO evaporation source on the sheet resistance of ITO films deposited by IBAE and the effect of the annealing temperature on the change in the sheet resistance.

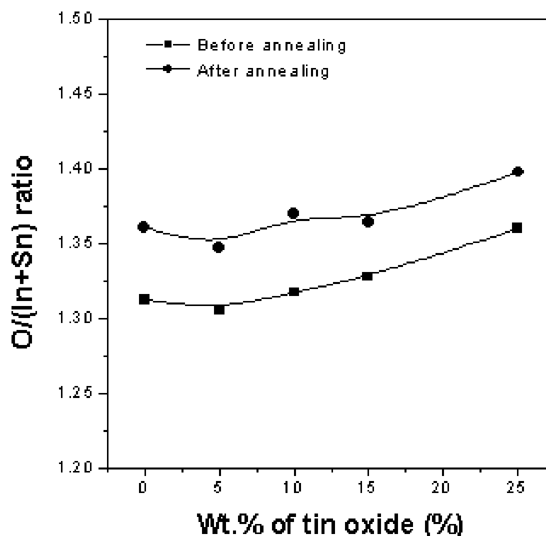

Fig. 2. O/(Sn + In) ratio in the film, as measured by XPS, as a function of tin oxide wt.% in the ITO evaporation source before and after the annealing at 300 °C for 1 h.

were optimized for each ITO source, as mentioned in the experimental section. As the figure show, the sheet resistance of as-deposited thin films increased with increasing tin concentration in the film even after the optimization. The electrical conductivities of the IO deposited at room temperature of the ITO thin films is mostly affected by the free electron concentration originating from ionized-oxygen-vacancies in the films. Therefore, the conductivity should strongly depend on the ratio of O/(Sn + In) in the film. In addition to the oxygen vacancies, the tin concentration in the deposited film can also affect the electrical conductivity of an ITO film deposited at room temperature. Tin atoms existing in amorphous ITO films remain as neutral impurities without donating electrons to the conduction band and decrease the conductivity by acting as additional scattering centers. Therefore, a higher tin concentration in an ITO deposited at room temperature results in a lower electrical conductivity [1, 13,19–23]. Through adequate thermal activation of the tin atoms, which may lead to the substitution of tin atoms at indium atomic sites, the neutral tin atoms can be ionized and donate one electron to the conduction band, which gives rise to improve electrical characteristics. In the case of IO, there are no tin atoms in the film; however, crystallization by annealing should also increase the conductivity of the film due to the increased carrier mobility. As Fig. 1 shows, an increase in the annealing temperature to 180 °C for IO films decreased the sheet resistance, possibly due to the recrystallization; however, a further increase in the temperature sharply increased the sheet resistance. This increase at high annealing temperatures over 180 °C is related to a decrease in the number of oxygen vacancies due to additional oxidation of the IO film during the annealing.

Fig. 2 shows the O/(Sn + In) ratio in the film, as

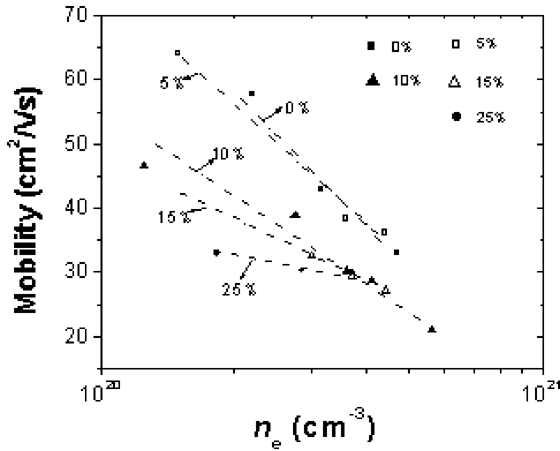

Fig. 3. Hall mobility of amorphous (as-deposited) IO and ITO thin films as a function of the free-electron concentration for various values of the tin-oxide wt.%.

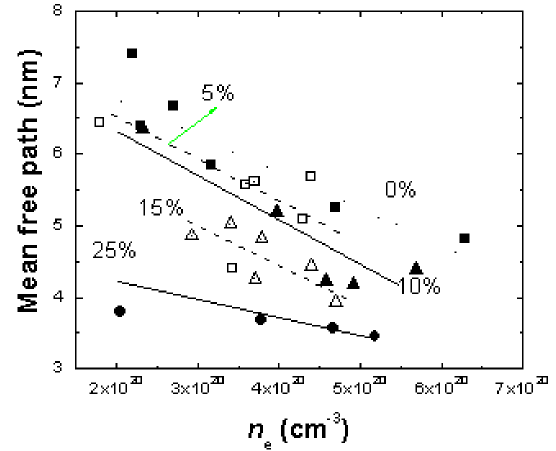

Fig. 4. Mean free path of amorphous IO and ITO thin films as a function of the free-electron concentration for various values of the tin oxide wt.%.

measured by XPS, as a function of the tin oxide wt.% in the ITO evaporation source before (as-deposited) and after annealing at 300 °C. As in the figure shows, annealing at 300 °C increases the ratio of O/(Sn + In) about 0.05 due to additional oxidation of the IO and the ITO films by the residual oxygen in the vacuum of 5 × 10^{-2} Torr during the annealing. Therefore, the increase in the sheet resistance of IO film during annealing at temperature above 180 °C can be ascribed to a decrease in the free-electron concentration originating from ionized oxygen vacancies due to additional oxidation. In the case of ITO, as Fig. 1 shows, even though annealing at high temperatures also caused an increase in the oxygen concentration to the value for the optimized as-deposited ITO thin film, the sheet resistance was decreased drastically by the annealing at temperature above 180 °C due to the activation of tin atoms and due to the recrystallization. Transitions in the IO and the ITO thin films from an amorphous to a crystalline structure were investigated using a transmission electron microscopy (TEM) by Muranaka *et al.* [24]. They reported a transition temperature of 160 °C for IO and 180 ∼ 190 °C for ITO thin films. A change of neutral Sn^{2+} to Sn^{4+} by substitution at the indium lattice site during annealing at temperature above 170 °C has also been reported by other researchers [1, 25–27] and agrees with our results for the change in sheet resistance with annealing.

The relationship between the carrier concentration and the carrier mobility for different tin concentrations was investigated to study the effect of the tin concentration in the ITO film on the carrier mobility. As Fig. 3 shows, increases in the carrier and the tin concentrations decrease the carrier mobility due to various scattering mechanisms. In the case of ITO, the scattering can be classified as 1) ionized impurity scattering, 2) neutral impurity scattering, 3) grain boundary scattering, and 4) lattice scattering. Among these, lattice scattering (4) is not a major scattering mechanism at low

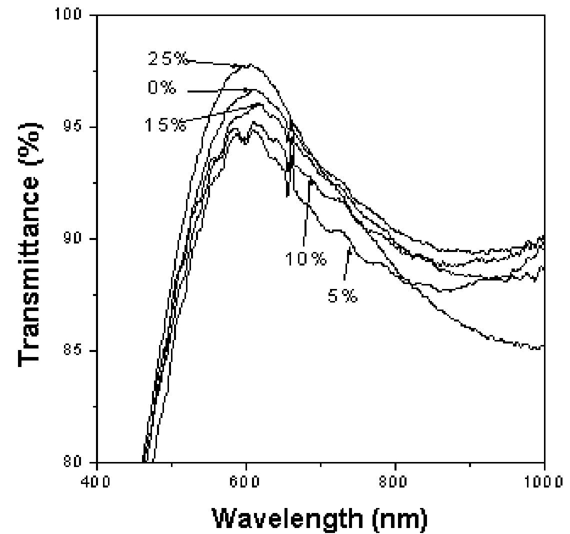

Fig. 5. Optical transmittances of as-deposited IO and ITO, as measured by a UV-visible spectrophotometer, as a function of the tin-oxide wt.%.

temperatures [26, 28–30] Also, because the grain size of room-temperature-deposited ITO is known to be above 10 nm [31], if the mean free path (MFP) of the electron in ITO is less than 10 nm, a grain boundary scattering can be ignored.

Fig. 4 shows the MFP calculated using the following equation suggested by Shigesato and Paine [31] for ITO with different tin concentrations;

$$V_F = (3\pi^2)^{1/3}[(h/2\pi)/m^*]n^{1/3} \quad (1)$$

$$t = V_F\tau = (3\pi^2)^{1/3}[(h/2\pi)/e^2]n^{2/3}\rho^{-1} \quad (2)$$

Here, n is the electron concentration, m* is the effective mass of an electron, τ is the relaxation time, ρ is the resistivity, V_F is the electron velocity, and t is the MFP. As in the figure shows, the calculated MFPs of IO and ITO deposited at room temperature were less than 4.5

Table 1. Characteristics of as-deposited and annealed IO and ITO thin films. Post-annealing was carried out at 300 °C in vacuum for 1 h.

SnO_2 wt.%		T (%)	Re (Ohm/eq.)	R_{aurf} (nm)	Optical bandgap Dir.	Optical bandgap Indir	O/(In + Sn)
0 %	As-depo	97	37	0.3	3.76	3.39	1.318
	Annealed		104	0.7	3.79	3.24	1.36
5 %	As-depo	95	38	0.75	3.753	3.364	1.306
	Annealed		28	0.87	3.833	3.3	1.347
10 %	As-depo	95	42	0.8	3.74	3.28	1.318
	Annealed		18	1.15	3.855	3.323	1.37
15 %	As-depo	96	48	0.76	3.736	3.338	1.328
	Annealed		19	0.79	3.853	3.364	1.364
25 %	As-depo	97	57	0.72	3.733	3.15	1.36
	Annealed		25	0.8	3.813	3.21	1.398

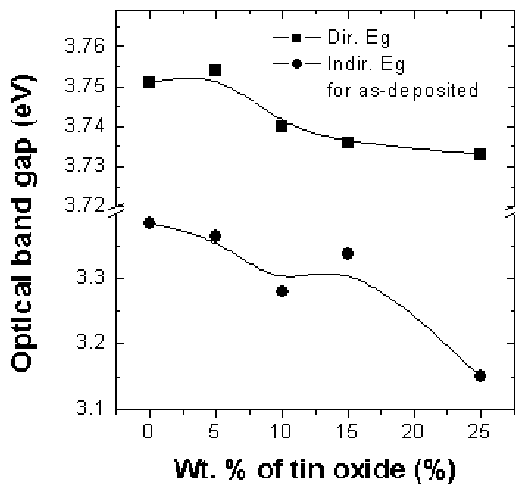

Fig. 6. Optical bandgaps of as-deposited IO and ITO as a function of the tin-oxide wt.% estimated using the results from a UV-visible spectrophotometer.

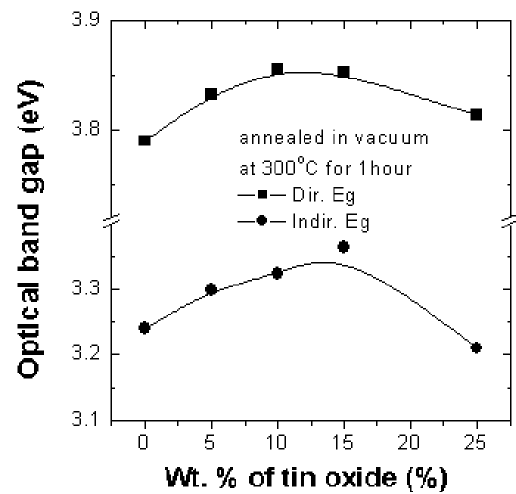

Fig. 7. Variation of the optical bandgaps with the tin-oxide wt.% for IO and ITO annealed at 300 °C in vacuum for 1 h.

nm and 7.5 nm, respectively. Due to the MFPs being smaller than the typical grain size, grain boundary scattering could be ignored under these experimental conditions. In the figure, a lower tin concentration appears to show a larger MFP for a similar electron concentration, which is due to tin atoms leading to neutral impurity scattering. It is difficult to determine the relative importance of neutral impurity scattering and ionized impurity scattering because the mobilities and the MFPs shown in Fig. 3 and 4, respectively, depend significantly on both tin-oxide wt.% and the electron concentration, which are related to neutral impurity scattering and ionized impurity scattering, respectively. However, the electron concentration appears to be more important than the tin wt.% at the low values of tin wt.%, even though the effect of the tin wt.% on the mobility increases at the high values of the tin wt.%.

Fig. 5 shows the optical transmittances of as-deposited IO and ITO films, as measured by a UV-visible spectrophotometer, as a function of the tin-oxide wt.% in the ITO evaporation source. The optical transmittances at 550 nm were higher than 90 % for all of the as-deposited films, and the change with tin concentration was not significant. In fact, the optical transmittance depended more on the oxygen concentration or O/(Sn + In) rather than on the tin concentration in the film, as shown in previous studies [6–9]. When the optical transmittances of the annealed IO and ITO thin films were measured, the annealed films appeared to be more transparent than the as-deposited films due to the higher oxygen concentrations in the annealed films (not shown).

It has been well known that the optical bandgap of IO and ITO films can be varied by using the deposition technique or the deposition conditions. Fig. 6 shows the optical bandgaps of as-deposited IO and ITO as functions

of the tin oxide wt.% estimated from the results of the UV-visible spectrophotometer. The bandgaps of room-temperature-deposited or annealed ITO are known to be in the range from 3.7 to 4.2 eV for the direct bandgap and from 2.8 to 3.4 eV for the indirect bandgap. The indirect bandgap calculated for an electron concentration of $10^{19}/cm^3$ is less than 3.0 eV, and that calculated for $6 \times 10^{20}/cm^3$ is 3.4 eV [32]. From this, an electron concentration of about $10^{20}/cm^3$ was estimated for our thin films. The increase in the optical bandgap with the number of free electrons in ITO is known as the Moss-Burnstein shift [32]. On the other hand, the decrease in the bandgap with the tin oxide wt.% in the figure is due to a decrease in the free-electron concentration with increasing tin impurity. Fig. 7 shows the optical bandgaps of IO and ITO films annealed at 300 °C in vaccum for 1h. The optical bandgap increased with the tin oxide wt.% and showed a maximum at 10 – 15 wt.% of tin oxide due to an increase in the free-electron concentration in the film during the annealing by the substitution of Sn^{2+} for Sn^{4+}. The decrease at 25 wt.% of tin oxide appears to be from the large number of tin atoms still remaining as impurities, Sn^{2+}.

The characteristics of the IO and the ITO films used in this study are briefly summarized in Table 1. The RMS surface roughness of the as-deposited and the annealed (300 °C) IO and ITO was measured using AFM, and the results are shown in the table. In general, the annealing process increased the grain size of the film and the top of the grain became rounder similar to the results reported by Adurodija *et al.* [19]. As Table 1 shows, the RMS roughness of the IO and ITO as-deposited by IBAE was less than 1 nm, and annealing increased the surface roughness. However, that of the annealed samples was less than 1.2 nm. The effect of the tin concentration in the film on the surface roughness for both as-deposited and annealed samples appeared not to be significant.

IV. CONCLUSIONS

In this study, the effects of the tin concentration in ITO thin films deposited at room temperature by using a dual oxygen IBAE technique, followed by vacuum annealing, on the electrical and the optical properties were investigated. The tin atoms in amorphous ITO thin films remained as neutral impurities and did not act as donors. Therefore, an increase in the tin concentration in the film decreased the electrical conductivity. However, annealing at temperature above 180 °C increased the conductivity for ITO films due to the activation of tin atoms by the substitution of Sn^{2+} for Sn^{4+}, donating electrons to the conduction band. In the case of IO, annealing at temperature above 180 °C decreased the conductivity due to a decrease in the number of oxygen vacancies in the film by additional oxidation during the annealing. The optical transmittances at 550 nm of the as-deposited IO and ITO thin films were higher than 90 %, and the tin concentration in the films did not affect the optical transmittance significantly. The surface roughness measured for the as-deposited IO and ITO thin films was lower than 1 nm. Annealing increased the surface roughness; however, the roughness was still lower than 1.2 nm.

REFERENCES

[1] J. R. Bellingham, W. A. Phillips and C. J. Adkins, J. Phys.: Condens. Matt. **2**, 6207 (1990).

[2] J. Ma, D. Zhang, J. Zhao, C. Tan, T. Yang and H. Ma, Appl. Surf. Sci. **151**, 239 (1999).

[3] J. George and C. S. Menon, Surface and Coatings Technology **321**, 45 (2000).

[4] J. A. Dobrowolski, F. C. Ho, D. Menagh, R. Simpson and A. Waldorf, Appl. Opt. **26**, 5204 (1987).

[5] S. Laux, N. Kaiser, A. Zoler, R. Gozelmann, H. Lauth and H. Bernitzki, Thin Solid Films **335**, 1 (1998).

[6] J. S. Kim, J. W. Bae, H. J. Kim, N. E. Lee, G. Y. Yeom and K. H. Oh, Thin Solid Films **377-378**. 103 (2000).

[7] J. W. Bae, H. J. Kim, J. S. Kim, N. E. Lee and G. Y. Yeom, Vacuum **56**, 77 (2000).

[8] J. W. Bae, H. J. Kim J. S. Kim, Y. H. Lee, N. E. Lee, G. Y. Yeom and Y. W. Ko, Surface and Coatings Technology **131**, 196 (2000).

[9] J. T. Lim, N. G. Cho, C. H. Jeong, J. H. Lee, J. H. Lim and G. Y. Yeom, J. Korean Phys. Soc. **47**, 142 (2005).

[10] D. G. Lim, I. Lee and J. Yi, J. Korean Phys. Soc. **49**, 41 (2001).

[11] R. Koshi-ishi, P. K. Song, Y. Shigesato and T. Kawashima, J. Ohsako, Transaction of the Materials Research Society of Japan **25**, 341 (2000).

[12] P. K. Song, H. Akao, M. Kamei, Y. Shigesato and I. Yasui, Jpn. J. Appl. Phys. **38**, 5224 (1999).

[13] H. Aharoni, T. J. Coutts, T. Gessert, R. Dhere and L. Schilling, J. Vac. Sci. Technol. A **3**, 428 (1986).

[14] J. C. C. Fan, Appl. Phys. Lett. **34**, 515 (1979).

[15] D. H. Kim, Y. G. Han, J. S. Cho and S. K. Koh, Thin Solid Films **377-378**, 81 (2000).

[16] Y. H. Son, J. H. Lee and H. J. Kim, J. Korean Phys. Soc. **42**, 814 (2003).

[17] X. W. Sun, H. C. Huang and H. S. Kwok, Appl. Phys. Lett. **68**, 2663 (1996).

[18] H. Kim, C. G. Gilmore and A. Pique, J. Appl. Phys. **86**, 6451 (1999).

[19] F. O. Adurodija, H. Izumi, T. Ishihara, H. Yoshioka and M. Motoyama: J. Vac. Sci. & Technol. A **18**, 814 (2000).

[20] T. A Gessert, D. L Williamson, T. J. Coutts, A. J. Nelson, K. M. Jones, R. G. Dhere, H. Aharoni and P. Zurcher, J. Vac. Sci. & Technol. A **5**, 1314 (1987).

[21] R. G. Dhere, T. A Gessert, L. L. Schiling, A. J. Nelson, K. M. Jones, H. Aharoni and T. J. Coutts, Sol. Cell. **21**, 281 (1987).

[22] Z. Ovadyahu, B. Ovryn and H. W. Kraner, J. Electrochem. Soc. **130**, 917 (1983).

[23] I. Hamberg, C. G. Granqvist, K. F. Berggren, B. E. Sernelius and L. Engstrom, Phys. Rev. B **30**, 3240 (1984).

[24] S. Muranaka, Y. Bando and T. takada, Thin Solid Films **25**, 355 (1987).

[25] M. Mizuhashi, Thin Solid Films **70**, 91 (1980).
[26] G. Frank and H. Kostlin, Appl. Phys. A **27**, 197 (1982).
[27] Y. Shigesato and D. C. Paine, Appl. Phys. Lett. **62**, 1268 (1993).
[28] G. Frank and H. Kostlin: Appl. Phys. A **27**, 197 (1982).
[29] T. M Ratcheva, M. D. Nanova, L. V. Vassilev and M. G. Mikhailov: Thin Solid Films **139**, 189 (1986).
[30] D. L. Dexter and F. Seitz: Phys. Rev. **86**, 864 (1952).
[31] R. B. Dingle: Phil. Mag. **46**, 831 (1955).
[32] H. L. Hartnagel, *Semiconducting Transparent Thin Films, Institute of Physics Publishing, Ltd.* (Bristol and Philadelphia, 1995), Chap. 4.